MULTISCALE MULTI-DIMENSIONAL EXPLICIT A-POSTERIORI ERROR ESTIMATION FOR FLUID DYNAMICS

Guillermo Hauke, Mohamed H. Doweidar and Daniel Fuster

Centro Politecnico Superior Zaragoza
Area de Mecanica de Fluidos
C/Maria de Luna 3, 50.019 Zaragoza, Spain
e-mail: ghauke@unizar.es

Key words: Fluid Dynamics, A-Posteriori Error Estimation, Hyperbolic Problems

Abstract. *A-posteriori error estimation of convection-dominated and hyperbolic flow problems remains one of the largest challenges in computational mechanics. The available techniques are either non-robust or computationally involved. This paper presents the multi-dimensional application of explicity a-posteriori error estimation based on the variational multiscale theory. In particular, adequate norms are proposed for the computation of the error and the proper error intrinsic scales are calculated for the bilinear quad. Furthermore, the model considers the element-interface error along the element edges, correcting the error prediction in the diffusive limit.*

1 INTRODUCTION

Although a-posteriori error estimation for solid mechanics has received much attention [1], a-posteriori error estimation of convection-dominated and hyperbolic flow problems remains one of the largest challenges in computational mechanics. The available techniques are either non-robust (that is, the predicted error does not converge uniformly to the exact error [19, 20]) or computationally involved (i.e. requiring the solution of additional partial differential equations, like in [21, 14]).

The variational multiscale approach offers a novel point of departure to set up strategies for the development of efficient and accurate a-posteriori error estimators [17, 10]. This approach has been shown exact for the class of edge-exact solutions and may deliver the error in the norm of choice [11, 12, 13].

In this paper, previous work is extended to multi-dimensional flows. And although the theory is not exact in this case, [18] shows that, for the class of methods stemming from H_0^1 projection or optimizaction (like stabilized methods), the error distribution is practically local. This strategy is, therefore, well suited for hyperbolic solutions computed with stabilized methods. In particular, adequate norms are proposed for the computation

of the error and the error intrinsic scales for the bilinear quad are calculated from element Green's functions.

In order to improve the error prediction capabilities in the diffusive limit, the present model considers the element-interface errors along the element edges. As a consequence, the previously reported error under-prediction out of the advection-dominated regime is cured. Furthermore, the present technique can be applied also to the elliptic limit.

2 THE VARIATIONAL MULTISCALE APPROACH TO ERROR ESTIMATION

2.1 The abstract problem

Consider a spatial domain Ω with boundary Γ. The strong form of the boundary-value problem consists of finding $u : \Omega \to \mathbb{R}$ such that for the given essential boundary condition $\mathbf{g} : \Gamma_g \to \mathbb{R}$, the natural boundary condition $h : \Gamma_h \to \mathbb{R}$, and forcing function $f : \Omega \to \mathbb{R}$, $f \in L_2$ (if $\Gamma_h = \emptyset$, $f \in H^{-1}$), the following equations are satisfied

$$
\begin{aligned}
\mathcal{L}u &= f && \text{in} \quad \Omega \\
u &= \mathbf{g} && \text{on} \quad \Gamma_g \\
\mathcal{B}u &= h && \text{on} \quad \Gamma_h
\end{aligned}
\tag{1}
$$

where $\mathcal{L}$ is in principle a second-order differential operator and $\mathcal{B}$ an operator acting on the boundary, emanating from integration-by-parts of the weak form.

2.2 The error estimation paradigm

The variational multiscale method [15] introduces a sum decomposition of the *exact solution* $u \in \mathcal{S} \subset H^1$ into the *finite element solution* (resolved scales) $\bar{u}$ and the *error* (unresolved scales) u',

$$
u = \bar{u} + u'
\tag{2}
$$

Typically $\bar{u}$ belongs to a finite element space $\bar{\mathcal{S}}$ with Ω^e, $e = 1, \ldots, n_{\text{el}}$ disjoint elements. The union of element interiors is denoted by $\widetilde{\Omega} = \cup_e^{n_{\text{el}}} \Omega^e$ whereas the inter-element boundaries, by $\widetilde{\Gamma} = \cup_e^{n_{\text{el}}} \Gamma^e \setminus \Gamma$ with Γ^e the element boundary. Accordingly, the error $u' \in \mathcal{S}'$ with $\mathcal{S}' = \mathcal{S} \setminus \bar{\mathcal{S}}$.

Then, the error of the numerical computation can be calculated by the following paradigm [17, 10]

$$
\begin{aligned}
u'(x) = \ &- \int_{\widetilde{\Omega}_y} g'(x,y)\, (\mathcal{L}\bar{u} - f)(y)\, \mathrm{d}\Omega_y - \int_{\widetilde{\Gamma}_y} g'(x,y)\, ([\![\mathcal{B}\bar{u}]\!])(y)\, \mathrm{d}\Gamma_y \\
&- \int_{\Gamma_{hy}} g'(x,y)\, (\mathcal{B}\bar{u} - h)(y)\, \mathrm{d}\Gamma_y
\end{aligned}
\tag{3}
$$

where $g'(x,y) \in \mathcal{S}' \times \mathcal{S}'$ is the Green's function of the *fine-scale* problem [15, 17], $[\![\cdot]\!]$ is the jump operator [16, 17] and $x, y \in \Omega^e$.

The fine-scale Green's function is the distribution that characterizes the behavior of the numerical error, and emanates from the proper projection of the global Green's function. Therefore, it depends on the operator (with the corresponding geometry and boundary conditions), on the finite element space and on the method (or projector) [18].

The error representation (3) can be split into errors estemming from element interior residuals and boundary element residuals, namely

$$u'(x) = u'_{\text{int}}(x) + u'_{\text{bnd}}(x) \tag{4}$$

Therefore, using the triangle inequality we can write

$$||u'(x)|| \le ||u'_{\text{int}}(x)|| + ||u'_{\text{bnd}}(x)|| \tag{5}$$

2.3 A model for the error distribution

2.3.1 Element interior error

The computation of the exact error requires full knowledge of the fine-scale Green's function, which can be analytically or computationally involved. However, for certain types of variational methods, such as stabilized methods, the error distribution is practically local [18]. For these methods, the fine-scale Green's function can be approximated by the element Green's function $g_e(x, y)$, which for linear elements, satisfies within each element

$$\begin{cases} \mathcal{L}g_e &= \delta_y & \text{in} & \Omega^e \\ g_e &= 0 & \text{on} & \Gamma^e \end{cases} \tag{6}$$

where $\delta_y(x) = \delta(x - y)$ represents the Dirac delta distribution.

Following [10, 11, 12] the error due to element interiors is modeled as

$$u'_{\text{int}}(x) \approx -\int_{\Omega_y^e} g_e(x, y) \, (\mathcal{L}\bar{u} - f)(y) \, \mathrm{d}\Omega_y \qquad \text{on } \Omega^e \tag{7}$$

The preceeding paradigm (7) is exact for element-edge-exact solutions. This is the case of one-dimensional linear problems solved with stabilized methods or that of one-dimensional Poisson problems solved with the Galerkin method.

By Hölders inequality (see Brenner and Scott [2]),

$$|u'_{\text{int}}(x)| \le ||g_e(x, y)||_{L_p(\Omega_y^e)} \, ||\mathcal{L}\bar{u} - f||_{L_q(\Omega^e)} \tag{8}$$

with $1 \le p, q \le \infty$, $1/p + 1/q = 1$. Taking the L_r norm,

$$||u'_{\text{int}}(x)||_{L_r(\Omega^e)} \le \left|\left| \, ||g_e(x, y)||_{L_p(\Omega_y^e)} \right|\right|_{L_r(\Omega_x^e)} ||\mathcal{L}\bar{u} - f||_{L_q(\Omega^e)} \tag{9}$$

3

2.3.2 Element boundary error

The inter-element boundary errors are approximated within each element as

$$u'_{\text{bnd}}(x) \approx - \int_{\Gamma^e_y} g'(x,y) \, (\llbracket \mathcal{B}\bar{u} \rrbracket)(y) \, \mathrm{d}\Gamma_y \qquad \text{on } \Omega^e \tag{10}$$

where the jump definition has been formally extended to encompass the natural boundary condition residual,

$$\llbracket \mathcal{B}\bar{u} \rrbracket = \begin{cases} \mathcal{B}\bar{u} - h & \text{on } \Gamma^e \cap \Gamma_h \\ 0 & \text{on } \Gamma^e \cap \Gamma_g \end{cases} \tag{11}$$

Again, by Hölders inequality

$$|u'_{\text{bnd}}(x)| \leq ||g'(x,y)||_{L_p(\Gamma^e_y)} \, ||\llbracket \mathcal{B}\bar{u} \rrbracket||_{L_q(\Gamma^e)} \tag{12}$$

with $1 \leq p, q \leq \infty$, $1/p + 1/q = 1$ and taking the L_r norm,

$$||u'_{\text{bnd}}(x)||_{L_r(\Omega^e)} \leq \left| \left| \, ||g'(x,y)||_{L_p(\Gamma^e_y)} \right| \right|_{L_r(\Omega^e_x)} ||\llbracket \mathcal{B}\bar{u} \rrbracket||_{L_q(\Gamma^e)} \tag{13}$$

2.3.3 Norms of interest

Because the Green's function may not be a very smooth in multidimensional applications, the choice $p = 1$ and $q = \infty$ is of particular interest. Then, typical choices for r are $r = 1$ or $r = 2$. In this case, if $g_e(x,y)$ does not change sign in Ω^e,

$$\left| \left| \, ||g_e(x,y)||_{L_1(\Omega^e_y)} \right| \right|_{L_r(\Omega^e_x)} = ||b_0(x)||_{L_r(\Omega^e_x)} \tag{14}$$

where the function $b_0^e(x)$ is a *residual-free bubble* [3, 4, 7, 5], defined as

$$b_0^e(x) = \int_{\Omega^e} g_e(x,y) \, \mathrm{d}\Omega_y \tag{15}$$

also solution of the problem

$$\begin{cases} \mathcal{L}b_0^e = 1 & \text{in } \Omega^e \\ b_0^e = 0 & \text{on } \Gamma^e \end{cases} \tag{16}$$

Using residual-free bubbles as error estimators was studied in [22]. Then, the error time scales can be defined as [11]

$$\tau_{L_1} = \frac{1}{\text{meas}(\Omega^e)} ||b_0(x)||_{L_1(\Omega^e)} \tag{17}$$

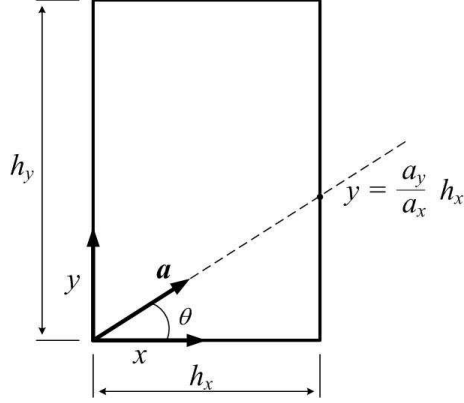$$\tau_{L_2} = \frac{1}{\text{meas}(\Omega^e)^{1/2}} ||b_0(x)||_{L_2(\Omega^e)} \tag{18}$$

Figure 1: Rectangular element.

so

$$\left|\left|\ ||g_e(x,y)||_{L_1(\Omega^e_y)}\right|\right|_{L_1(\Omega^e_x)} = \tau_{L_1}\ \mathrm{meas}(\Omega^e) \tag{19}$$

$$\left|\left|\ ||g_e(x,y)||_{L_1(\Omega^e_y)}\right|\right|_{L_2(\Omega^e_x)} = \tau_{L_2}\ \mathrm{meas}(\Omega^e)^{1/2} \tag{20}$$

Now, an analysis shows that the norm on Γ^e of the fine-scale Green's function can be approximated to the norm of the element Green's function in the domain Ω^e by,

$$\left|\left|\ ||g'(x,y)||_{L_1(\Gamma^e_y)}\right|\right|_{L_r(\Omega^e_x)} \approx \frac{1}{2}\frac{\mathrm{meas}(\Gamma^e)}{\mathrm{meas}(\Omega^e)}\left|\left|\ ||g_e(x,y)||_{L_1(\Omega^e_y)}\right|\right|_{L_r(\Omega^e_x)} \tag{21}$$

Further details will be given at the conference.

3   MULTIDIMENSIONAL ERROR SCALES FOR THE BILINEAR QUAD

In this section, we will consider the 2D error scales, with Cartesian coordinates x and y.

3.1   Hyperbolic limit

In the hyperbolic limit, the residual-free-bubble is the solution of the problem

$$\begin{cases} |\boldsymbol{a}|\nabla_a b^e_0 &= 1 \qquad \text{in} \quad \Omega^e \\ b^e_0 &= 0 \qquad \text{on} \quad \Gamma^e_{\text{in}} \end{cases} \tag{22}$$

which can be expressed as

$$b^e_0(x) = \begin{cases} \dfrac{y}{|\boldsymbol{a}|\sin\theta} & \qquad y < \frac{a_y}{a_x}x \\[2mm] \dfrac{x}{|\boldsymbol{a}|\cos\theta} & \qquad y > \frac{a_y}{a_x}x \end{cases} \tag{23}$$

For $h_y > h_x a_y / a_x$ (streamline below upper-right corner) the norms of $g_e(x, y)$ yield the corresponding error time scales,

$$
\tau_{L_1} = \frac{||b_0||_{L_1(\Omega^e)}}{\text{meas}(\Omega^e)} = \frac{h_{\text{flow}}}{2|\boldsymbol{a}|}
$$

$$
\tau_{L_2} = \frac{||b_0||_{L_2(\Omega^e)}}{\text{meas}(\Omega^e)^{1/2}} = \frac{h_{\text{flow}}}{\sqrt{3}|\boldsymbol{a}|} \sqrt{1 - \frac{1}{2} \frac{a_y}{a_x} \frac{h_x}{h_y}} \leq \frac{h_{\text{flow}}}{\sqrt{3}|\boldsymbol{a}|}
$$

where h_{flow} is the longest length of the element along the streamwise direction. This result, proved here rigoruosly for quads, was suggested by [9] for quads. A similar result was derived for the linear triangle in [4, 8]. For $a_y h_x << a_x h_y$, $\tau_{L_2} \approx \frac{h_{\text{flow}}}{\sqrt{3}|\boldsymbol{a}|}$. Let us recall that in 1D $\tau_{\text{flow}} = \tau_{L_1}$ [11].

3.2 Elliptic limit

In the elliptic limit, the residual-free-bubble is the solution of the problem

$$
\begin{cases}
\kappa \Delta b_0^e = 1 & \text{in} \quad \Omega^e \\[2mm]
b_0^e = 0 & \text{on} \quad \Gamma^e
\end{cases}
$$

which can be expressed as the series

$$
b_0^e(x) = \frac{16}{\pi^4 \kappa} \sum_{m=1(\text{odd})}^{\infty} \sum_{n=1(\text{odd})}^{\infty} \frac{1}{\frac{n^2}{h_x^2} + \frac{m^2}{h_y^2}} \frac{1}{nm} \sin \frac{n\pi}{h_x} x \sin \frac{m\pi}{h_y} y
$$

The error scales for $h_x = h_y$ are calculated as

$$
\tau_{L_1} = \frac{h_x^2}{24.81\kappa}
$$

$$
\tau_{L_2} = \frac{h_x^2}{24.24\kappa}
$$

4 NUMERICAL EXAMPLES

In this paper in order to validate the proposed error estimator, three different examples are shown. Two of them correspond to the hyperbolic and elliptic and limiting cases, and the third one to a mixed advection-diffusion problem.

The case study consists of a squared domain with Dirichlet boundary conditions. The boundary values on the left and top side are equal to 1 and the values on the right and bottom sides, 0. Besides, in the left and top sides, the boundary condition decreases linearly from 1 to 0. The chosen lenght for this ramp is equal to the distance between nodes of the rough mesh, which has an element length of $h_x = 0.1$. The aim of establishing this
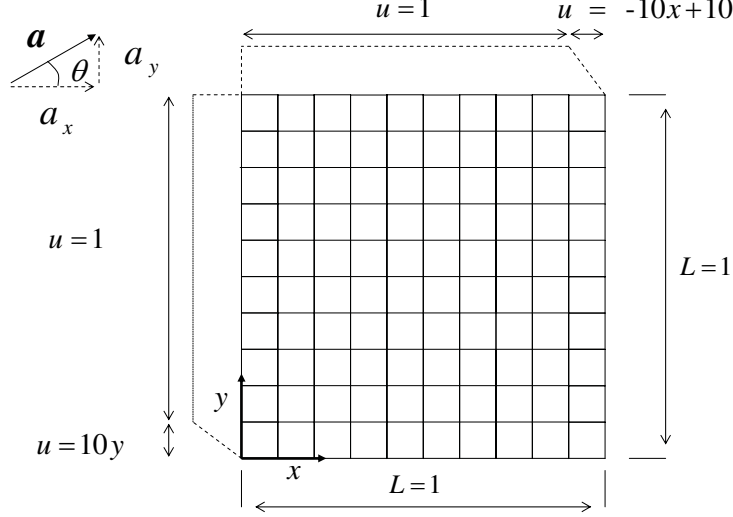
Figure 2: Problem schematic.

condition is to avoid discontinuities at the corners and to solve exactly the same problem for every mesh used along the validation.

There have been used structured meshes with three types of elements: quads, triangles with the diagonal in the flow direction and triangles with the diagonal in the perpendicular direction to the flow.
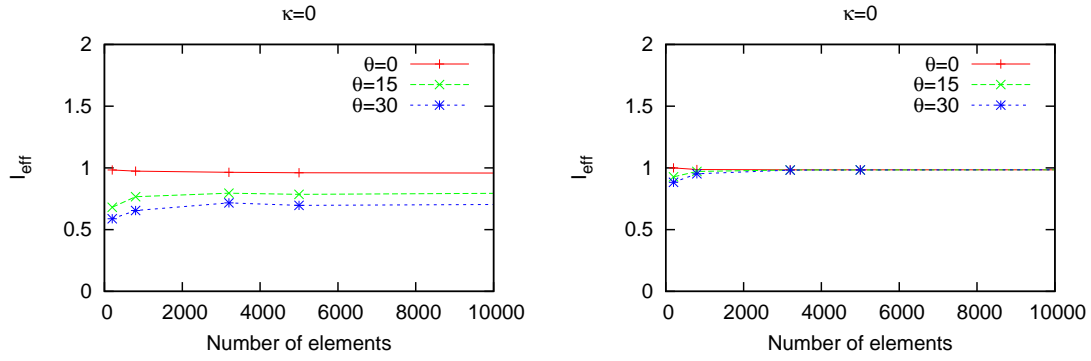
For all the examples, the following values of τ are used:

$$
\begin{aligned}
\tau_{\text{flow}} &= \min\left(\frac{h_{\text{flow}}}{2|\boldsymbol{a}|}; \frac{h_x^2}{12\kappa}\right) \\
\tau_{L_1} &= \min\left(\frac{h_{\text{flow}}}{2|\boldsymbol{a}|}; \frac{h_x^2}{24.81\kappa}\right) \\
\tau_{L_2} &= \min\left(\frac{h_{\text{flow}}}{\sqrt{3}|\boldsymbol{a}|}; \frac{h_x^2}{24.24\kappa}\right)
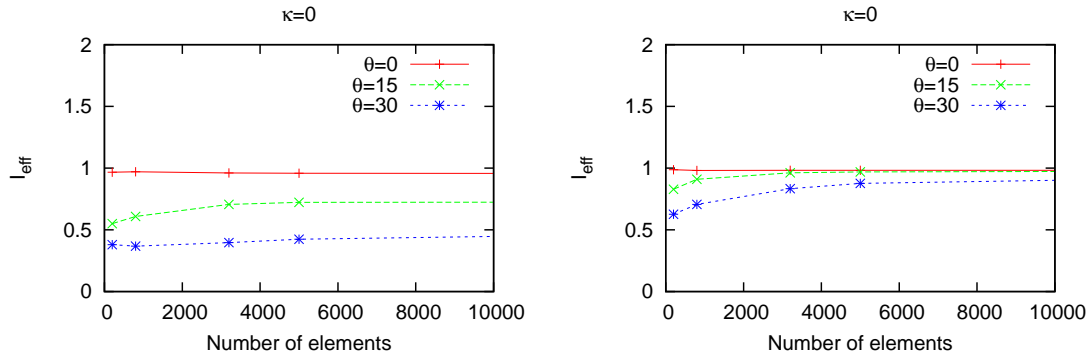\end{aligned}
$$

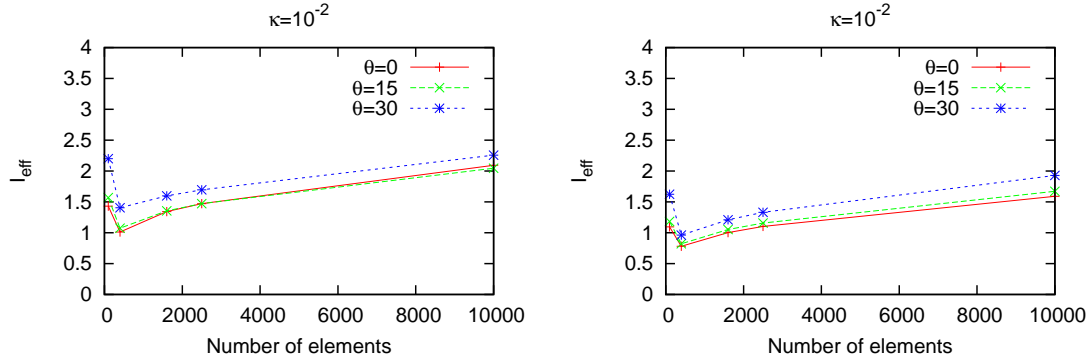Figs. 3-5 show the efficiencies for all the cases.
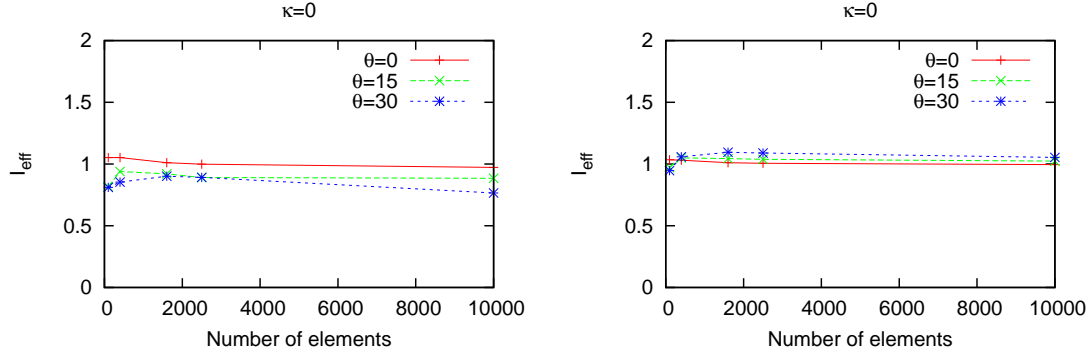
7

(a) Quads

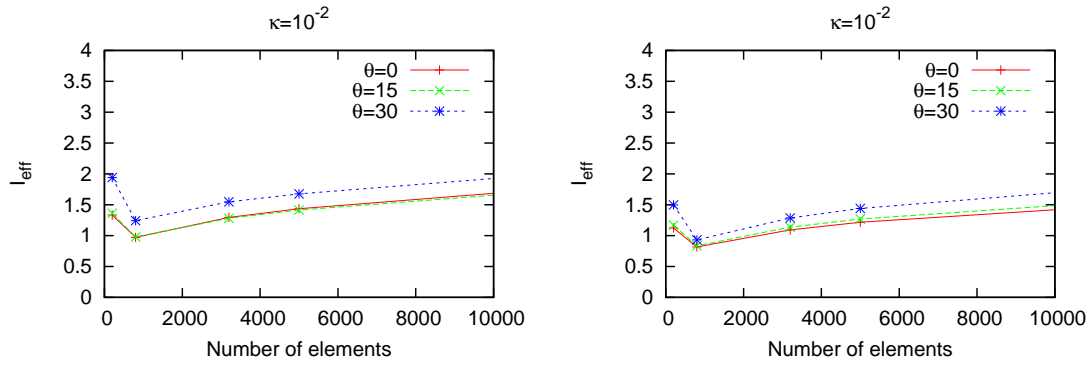(b) Triangles with the diagonal in the flow direction

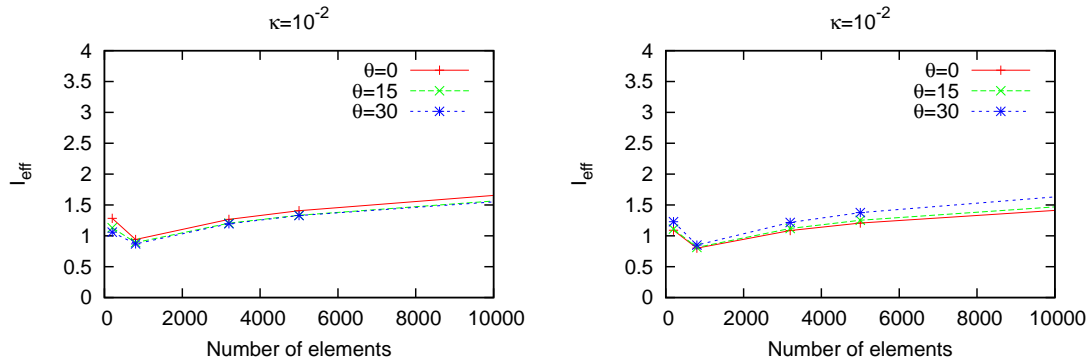(c) Triangles with the diagonal perpendicular to the flow direction

Figure 3: Efficiencies for the L_1 (left) and L_2 (right) norms. Advection dominated problem.
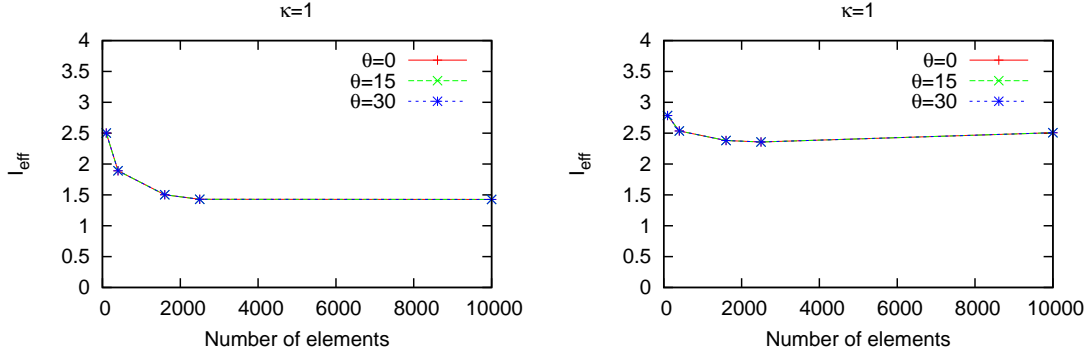
(a) Quads

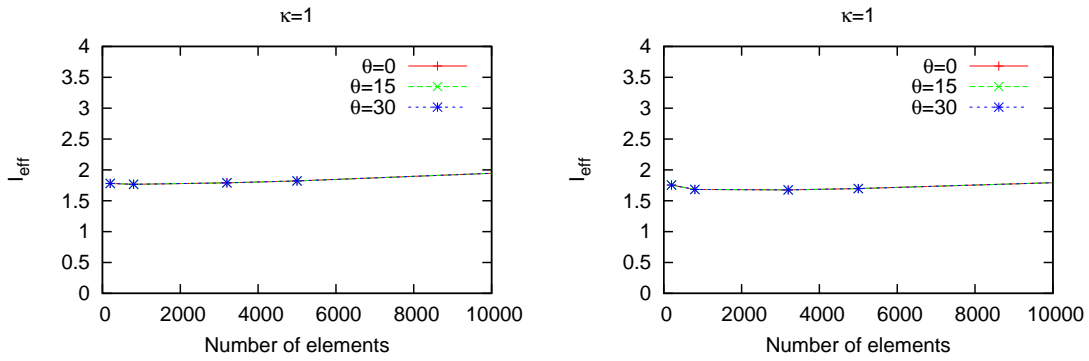(b) Triangles with the diagonal in the flow direction

(c) Triangles with the diagonal perpendicular to the flow direction

Figure 4: Efficiencies for the L_1 (left) and L_2 (right) norms. Advection-diffusion problem.

(a) Quads

(b) Triangles with the diagonal in the flow direction

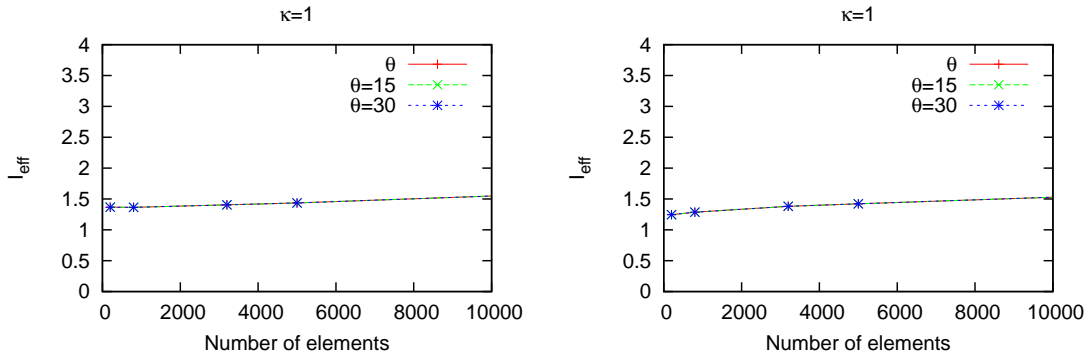(c) Triangles with the diagonal perpendicular to the flow direction

Figure 5: Efficiencies for the L_1 (left) and L_2 (right) norms. Pure diffusion problem.

5   CONCLUSIONS

An explicit a-posteriori error estimator has been developed from the variational multiscale framework. The technique includes both, interior element residuals and inter-element residuals. The error time scales (error constants) have been obtained explicitly from element Green's functions.

The method has been tested in the hyperbolic limit, in the elliptic limit and in a advection-diffusion problem. The results show efficiencies very close to one in all the cases. Only for hyperbolic problems and triangles with the diagonal normal to the velocity direction there is a slight lose of efficiency as the flow angle deviates from zero.

Thus, the present technique is very efficient and well suited for advection-diffusion problesms including both, the hyperbolic and elliptic limits.

REFERENCES

[1] M. Ainsworth and J.T. Oden. *A posterior error estimation in finite element analysis*, John Wiley & Sons, (2000).

[2] S.C. Brenner and L.R. Scott. *The mathematical theory of finite element methods*, second edition, Springer-Verlag, (2002).

[3] F. Brezzi and M.O. Bristeau and L. P. Franca and M. Mallet and G. Rogé. *A relationship between stabilized finite element methods and the Galerkin method with bubble functions*, Comput. Meth. Appl. Mech. Engrng., **96**, 117–129, (1992).

[4] F. Brezzi and A. Russo. *Choosing bubbles for advection-diffusion problems*, Mathematical Models and Methods in Applied Sciences, **4**, 571-587, (1994).

[5] F. Brezzi and L.P. Franca and T.J.R. Hughes and A. Russo. $b = \int g$, Comput. Meth. Appl. Mech. Engrng., **145**, 329–339, (1997).

[6] L.P. Franca and S.L. Frey and T.J.R. Hughes. *Stabilized finite element methods: I. Application to the advective-diffusive model*, Comput. Meth. Appl. Mech. Engrng., **95**, 253–276, (1992).

[7] L.P. Franca and A. Russo. *Deriving Upwinding, Mass Lumping and Selective Reduced Integration by Residual-Free Bubbles*, Applied Mathematics Letters, **9**, 83-88, (1996).

[8] L.P. Franca and A. Russo. *Recovering SUPG using PetrovGalerkin formulations enriched with adjoint residual-free bubbles*,Comput. Meth. Appl. Mech. Engrng., **182**, 333–339 (2000).

[9] L.P. Franca and F. Valentin. *On an improved unusual stabilized finite element method for the advective-reactive-diffusive equation*, Comput. Meth. Appl. Mech. Engrng., **190**, 1785-1800 (2000).

[10] G. Hauke and M.H Doweidar and M. Miana. *The Multiscale Approach to Error Estimation and Adaptivity, Comput. Meth. Appl. Mech. Engrng.*, **195**, 1573–1593 (2006).

[11] G. Hauke and M.H Doweidar and M. Miana. *Proper Intrinsic scales for a-posteriori Multiscale Error Estimation, Comput. Meth. Appl. Mech. Engrng.*, **195**, 3983–4001 (2006).

[12] G. Hauke and M.H Doweidar. *Intrinsic Scales and a Posteriori Multiscale Error Estimation for Piecewise-Linear Functions and Residuals, Int. J. Comput. Fluid Dynamics*, accepted.

[13] G. Hauke and M.H Doweidar and D. Fuster and A. Gomez and J. Sayas. *Application of Variational a-Posteriori Multiscale Error Estimation to Higher-Order Elements*, Computational Mechanics, DOI: 10.1007/s00466-006-0048-7, (2006).

[14] P. Houston and R. Rannacher and E. Süli. *A posteriori error analysis for stabilized finite element approximations of transport problem*, Comput. Methods Appl. Mech. Engrg., **190**, 1483–1508, (2000).

[15] T.J.R. Hughes. *Multiscale phenomena: Green's functions, the Dirichlet-to-Neumann formulation, subgrid scale models, bubbles and the origins of stabilized methods, Comput. Meth. Appl. Mech. Engrng.*, **127**, 387–401, (1995).

[16] T.J.R. Hughes. *The finite element method:Linear static and dynamic finite element analysis*, Dover Publications, (2000).

[17] T.J.R. Hughes and G.R. Feijoo and L. Mazzei and J.B. Quincy. *The variational multiscale method: A paradigm for computational mechanics, Comput. Meth. Appl. Mech. Engrng.*, **166**, 3–24, (1998).

[18] T.J.R. Hughes and G. Sangalli. *Variational multiscale analysis: the fine-scale Green's function, projection, optimization, localization and stabilized methods*, ICES Report 05-46 (2005). Submitted to SINUM.

[19] V. John. *A numerical study of a posteriori error estimators for convection-diffusion equations*, Comput. Methods Appl. Mech. Engrg., **190**, 757–781, (2000).

[20] A. Papastavrou and R. Verfürth,. *A posteriori error estimators for stationary convection-diffusion problems: a computational comparison*, Comput. Methods Appl. Mech. Engrg., **189**, 449–462, (2000).

[21] R. Rannacher. *A posteriori error estimation in least-squares stabilized finite element schemes*,Comput. Methods Appl. Mech. Engrg., **166**, 99–114, (1998).

[22] A. Russo. *A posteriori error estimators via bubble functions*, Mathematical Models and Methods in Applied Sciences, **1**, 33-41, (1996).